

1 **GABAergic neurons in the olfactory cortex projecting to the lateral hypothalamus**
2 **in mice**

3

4 Koshi Murata^{1,2,3}, Tomoki Kinoshita¹, Yugo Fukazawa^{1,2,4}, Kenta Kobayashi⁵, Kazuto
5 Kobayashi⁶, Kazunari Miyamichi⁷, Hiroyuki Okuno⁸, Haruhiko Bito⁹, Yoshio Sakurai³,
6 Masahiro Yamaguchi¹⁰, Kensaku Mori¹¹, and Hiroyuki Manabe³

7 1. Division of Brain Structure and Function, Faculty of Medical Sciences, University of
8 Fukui, Fukui 910-1193, Japan

9 2. Life Science Innovation Center, Faculty of Medical Science, University of Fukui,
10 Fukui 910-1193, Japan

11 3. Laboratory of Neural Information, Graduate School of Brain Science, Doshisha
12 University, Kyoto 610-0394, Japan

13 4. Research Center for Child Mental Health Development, Faculty of Medical Sciences,
14 University of Fukui, Fukui 910-1193, Japan

15 5. Section of Viral Vector Development, National Institute for Physiological Sciences,
16 Aichi 444-8585, Japan

17 6. Department of Molecular Genetics, Institute of Biomedical Sciences, Fukushima
18 Medical University School of Medicine, Fukushima 960-1295, Japan

19 7. Laboratory for Comparative Connectomics, RIKEN Centre for Biosystems Dynamics
20 Research, Hyogo 650-0047, Japan

21 8. Department of Biochemistry and Molecular Biology, Kagoshima University Graduate
22 School of Medical and Dental Sciences, Kagoshima 890-8544, Japan

23 9. Department of Neurochemistry, Graduate School of Medicine, The University of
24 Tokyo, Tokyo 113-0033, Japan

25 10. Department of Physiology, Kochi Medical School, Kochi University, Kochi
26 783-8505, Japan

27 11. Department of Physiology, Graduate School of Medicine, The University of Tokyo,
28 Tokyo 113-0033, Japan

29

30 **Correspondence to**

31 **Hiroyuki Manabe, Ph.D.**

32 Laboratory of Neural Information, Graduate School of Brain Science, Doshisha
33 University, Kyoto 610-0394, Japan

34 Phone: +81-774-65-7181

35 Email: hmanabe@mail.doshisha.ac.jp

36

37 **Abstract**

38 Olfaction guides goal-directed behaviours including feeding. To investigate how central
39 olfactory neural circuits control feeding behaviour in mice, we performed retrograde
40 tracing from the lateral hypothalamus (LH), an important feeding centre. We observed a
41 cluster of retrogradely labelled cells distributed in the posteroventral region of the
42 olfactory peduncle. Histochemical analyses revealed that a majority of these
43 retrogradely labelled projection neurons expressed glutamic acid decarboxylase 65/67
44 (GAD65/67), but not vesicular glutamate transporter 1 (VGluT1). We named this region
45 with GABAergic projection neurons the ventral olfactory nucleus (VON) to
46 discriminate it from the conventional olfactory peduncle. VON neurons were less
47 immunoreactive for DARPP-32, a striatal neuron marker, in comparison to those in the
48 olfactory tubercle and nucleus accumbens, which distinguished the VON from the
49 ventral striatum. Fluorescent labelling confirmed synaptic contacts between VON
50 neurons and olfactory bulb projection neurons. Rabies-virus-mediated trans-synaptic
51 labelling revealed that VON neurons received synaptic inputs from the olfactory bulb,
52 other olfactory cortices, horizontal limb of the diagonal band, and prefrontal cortex.
53 Collectively, these results identified novel GABAergic projection neurons in the
54 olfactory cortex that can integrate olfactory sensory and top-down inputs and send
55 inhibitory output to the LH, which may contribute to forming odour-guided LH-related
56 behaviours.

57

58 **Introduction**

59 The central olfactory system translates odour information into motivated behaviours,
60 including appetite-based food approach and eating behaviours¹. Recent studies have
61 revealed neuronal circuit mechanisms by which odorants evoke specific behaviours,
62 such as fear responses to predator odours^{2,3} and attractive responses to social odours⁴.
63 However, it is still unclear how the central olfactory neural circuits control
64 feeding-related behaviours in mammals.

65 Odorants activate olfactory sensory neurons and coded by activation of specific
66 combinations of glomeruli in the olfactory bulb (OB), the first relay centre of the central
67 olfactory system⁵. Mitral cells and tufted cells (M/TCs) are projection neurons in the
68 OB. They convey odour information to several areas in the olfactory cortex which is
69 composed of the anterior olfactory nucleus (AON), tenia tecta, dorsal peduncular cortex,
70 anterior piriform cortex (APC), olfactory tubercle (OT), posterior piriform cortex (PPC),
71 cortical amygdaloid nuclei, and entorhinal cortex⁶.

72 We previously reported that c-fos activity increased in the anteromedial domain
73 of the OT when mice showed attractive responses to a learned odour cue that predicted
74 food⁷. The OT has indirect anatomical connections to the lateral hypothalamus (LH), an
75 important feeding centre^{8,9}, via the ventral pallidum¹⁰. Knowledge of neural pathways
76 from the olfactory cortex to the LH is crucial to identify how olfactory information is
77 translated into feeding-related behaviours. Price et al. examined the neural connections
78 between the central olfactory system and the LH in rats¹¹, and reported that several parts
79 of the olfactory cortex have axonal projections to the LH. Since then, however, no
80 neuroanatomical studies have addressed how olfactory information is conveyed to the
81 LH in mammals.

82 Here, we re-examined the neural pathways from the central olfactory system to
83 the LH in mice using cholera toxin B subunit (CTB), and viral and genetic techniques to
84 trace neural circuits. In agreement with the previous study¹¹, we observed a subset of
85 retrogradely labelled cells clustered in a postero-ventral region of the olfactory peduncle.
86 Our analyses revealed that a majority of LH-projecting neurons in this region were
87 GABAergic neurons, in sharp contrast to the AON and ventral tenia tecta (VTT) where
88 principal neurons are glutamatergic. We also found that the GABAergic neurons
89 extended dendrites to layer I and received synaptic inputs from the olfactory bulb
90 neurons. These results suggest a novel population of GABAergic neurons in the
91 olfactory cortex projecting to the LH.

92

93 **Results**

94 **Retrograde tracer injection into the LH revealed a cluster of GABAergic neurons
95 in the olfactory peduncle**

96 To reveal neural pathways from the olfactory cortex to the LH, we injected a retrograde
97 tracer, CTB conjugated with Alexa 555, into the mouse LH. We targeted an area of the
98 LH where orexin neurons and melanin-concentrating hormone (MCH) neurons were
99 distributed (Fig. 1A), as both these neuronal subpopulations are involved in feeding
100 behaviours^{12,13}. CTB-labelled cells were widely distributed in the brain including the
101 prefrontal cortex (Fig. 1B, left). Guided by previous studies reporting that the olfactory
102 cortex has axonal projections to the LH¹¹, we found a cluster of CTB-labelled cells in an
103 area surrounded by the AON, APC, VTT, and OT (Fig. 1B right). The size of
104 CTB-labelled somata was smaller than that of principal neurons in the posterior part of
105 the AON (Figs. 1B and 2), suggesting that their neuronal subtypes differed from
106 principal neurons in the AON.

107 To examine whether the CTB-labelled cells were glutaminergic or GABAergic,
108 we performed *in situ* hybridization for mRNA of vesicular glutamate transporters
109 (VGluTs) and glutamic acid decarboxylase (GAD) 65/67 in this area (Fig. 2).
110 VGluT1-expressing cells were distributed in the dorsal edge of the area in which
111 CTB-labelled cells were clustered. We observed a cluster of GAD65/67-expressing cells
112 just above the rostral tip of the OT, which overlapped with the distribution of
113 CTB-labelled cells. VGluT2- and VGluT3-expressing cells were scarcely observed in
114 this area. We then directly examined expression of VGluT1 and GAD65/67 mRNAs in
115 CTB-labelled cells by double fluorescent labelling (Fig. 2B). VGluT1-expressing
116 CTB-labelled cells were distributed in the ventral border of the AON, and 7.8% of the

117 CTB-labelled cells were VGluT1-positive (n = 154 cells from two mice). In contrast,
118 84.6% of the CTB-labelled cells were GAD65/67-positive (n = 214 cells from three
119 mice), which suggested that principal neurons in this area were GABAergic. Projection
120 neurons in the olfactory cortex, except for the OT, are thought to be glutamatergic. This
121 cellular profile raised a possibility that the GABAergic CTB-labelled cells did not
122 belong to the conventional olfactory peduncle. We therefore temporarily named this
123 area the ventral olfactory nucleus (VON), because the cluster of GABAergic neurons
124 projecting to the LH was located just ventral to the AON.

125 One possible cellular profile of GABAergic neurons in the VON is medium
126 spiny neurons in the OT and nucleus accumbens (NAc), namely the ventral striatum^{14,15}.
127 To examine whether the CTB-labelled cells in the VON were different from medium
128 spiny neurons of the ventral striatum, we performed immunostaining for DARPP-32, a
129 marker for striatal neurons¹⁶, alongside CTB labelling (Fig. 3). CTB-labelled cells were
130 distributed in both DARPP-32 strongly immunoreactive and less immunoreactive
131 regions, which corresponded to the ventral striatum and VON, respectively. These
132 results support the idea that GABAergic neurons in the VON formed distinct cellular
133 populations from medium spiny neurons in the OT and NAc.

134

135 **Synaptic contacts from OB M/TCs to VON neurons**

136 Olfactory cortex is defined as those areas that receive direct synaptic inputs from
137 M/TCs, projection neurons in the OB⁶. To reveal synaptic contacts from M/TCs onto the
138 dendrites of VON neurons, we used a transgenic mouse line in which M/TCs were
139 labelled by tdTomato (Pcdh21-nCre; tdTomato Cre reporter line, Ai14^{17,18}). We injected
140 retrogradely-spreading adeno-associated virus (AAV) encoding EGFP

141 (AAVrg-CAG-EGFP¹⁹) into the LH of the transgenic mice (Figs. 4-5). EGFP-labelled
142 dendrites of the VON neurons were innervated by tdTomato-labelled axons of M/TCs
143 (Fig. 4A, B), suggesting that VON neurons receive axonal synaptic inputs in layer Ia of
144 the olfactory cortex. Notably, dendrites of VON neurons did not innervate DARPP-32
145 strongly immunoreactive regions, the NAc and OT (Fig. 4B).

146 We next performed immunostaining for VGluT1, a presynaptic marker of
147 M/TCs^{20,21}, and examined apposition of VGluT1 signals and dendrites of VON neurons
148 (Fig. 5). EGFP-labelled dendrites of VON neurons had spines (Figs. 4B and 5). Axonal
149 boutons of tdTomato-labelled M/TCs in layer Ia were apposed to dendritic spines of
150 VON neurons, which colocalised with VGluT1 immunoreactivity (arrowheads in Fig. 5,
151 lower panels). These results suggest that VON neurons receive glutamatergic inputs
152 from M/TCs, and support the idea that the VON is a part of the olfactory cortex.

153

154 **Trans-synaptic retrograde tracing from the VON using a modified rabies virus**

155 To further confirm whether the VON was a part of the olfactory cortex, namely whether
156 VON neurons received direct synaptic inputs from M/TCs in the OB, we performed
157 trans-synaptic labelling of VON neurons combining an EnvA-pseudotyped
158 glycoprotein-deleted rabies virus encoding EGFP (SAD-dG-EGFP+EnvA) with
159 AAV-mediated expression of the EnvA receptor (TVA) and rabies glycoprotein²²⁻²⁵.
160 This labelling also revealed input pathways to the VON neurons in whole brain regions.
161 To achieve selective initial infection of VON neurons by the rabies virus, we used the
162 neural pathway specific-tracing method (tracing the relationship between input and
163 output, TRIO²⁶). We first injected a retrograde Cre-coding lentiviral vector
164 (NeuRet-Cre²⁷) into the LH, and Cre-dependent AAV vectors encoding TVA-mCherry

165 and rabies G into the VON. Two weeks after the injection, we injected the modified
166 rabies virus (SAD-dG-EGFP+EnvA) into the VON (Fig. 6A).

167 Starter cells of TVA-mCherry(+) and EGFP(+) cells were observed in the VON
168 (Fig. 6B). We detected EGFP-labelled cells in the OB (Fig. 6C, upper left panel),
169 confirming that the VON neurons receive direct synaptic input from the OB.
170 EGFP-labelled cells were also distributed in the AON and OT (Fig. 6B, right panel),
171 APC (Fig. 6C, upper middle panel), orbitofrontal cortex (Fig. 6C, upper right panel),
172 medial prefrontal cortex (Fig. 6C, lower left panel), horizontal limb of the diagonal
173 band (Fig. 6C, lower middle panel), and PPC (Fig. 6C, lower right panel). These results
174 suggest that, in addition to the afferent input from the OB, VON receives inputs from
175 various areas of the olfactory cortex, a part of the diagonal band, and the prefrontal
176 cortex, as well as supporting the idea that the VON is a part of the olfactory cortex.

177

178 **Rabies virus-mediated trans-synaptic retrograde labelling from the LH to the VON**
179 CTB labelling could not discriminate whether the labelled cells had synaptic
180 connections to the postsynaptic neurons or whether their axon fibres were passing by in
181 the injection site²⁸. To address whether the VON neurons formed synaptic contacts in
182 the LH, we used trans-synaptic retrograde labelling from the LH with the modified
183 rabies virus as shown in Fig. 6. We injected Cre-encoding AAV and Cre-dependent
184 AAVs encoding TVA-mCherry and rabies glycoprotein into the LH, followed by
185 injection of the modified rabies virus (SAD-dG-EGFP+EnvA) into the LH²²⁻²⁵ (Fig. 7A).
186 Because trans-synaptic spread of the rabies virus is mediated by the rabies
187 glycoprotein²⁵, we compared efficacy of retrograde labelling with and without rabies G
188 expression in the LH. EGFP(+) cells were observed in the VON when we concomitantly

189 injected rabies G-coding AAV into the LH (Fig. 7B, upper panels). In contrast, EGFP(+)
190 cells were never observed in the VON in the absence of rabies G-coding AAV in the LH
191 (Fig. 7B, lower panels). TVA-mCherry(+) and EGFP(+) cells in the LH were observed
192 in cases with and without rabies G-coding AAV (data not shown). The results of rabies
193 glycoprotein-dependent retrograde spread of rabies virus supports the idea that neurons
194 in the VON form synaptic contacts in the LH.

195

196 **Discussion**

197 In this study, we examined the neural pathways from the olfactory cortex to the LH in
198 mice by retrograde tracing from the LH. We observed that a group of retrogradely
199 labelled cells was clustered in a postero-ventral region of the olfactory peduncle. Our
200 neuroanatomical and histochemical analyses revealed that this region predominantly
201 comprises GABAergic neurons, thereby distinguishing it from the AON and VTT in
202 which the principal neurons are glutamatergic. Furthermore, this region receives
203 synaptic inputs from the M/TCs. These results suggest a novel population of
204 GABAergic neurons in the olfactory cortex that project to the LH.

205 In accordance with the previous report by Price et al. in rats¹¹, we identified an
206 equivalent cluster of retrogradely-labelled cells in a posterior part of the olfactory
207 peduncle in mice surrounded by the AON, VTT, APC, and OT (Figs. 1B and 3).
208 Although it has been thought that this cluster of neurons belongs to the AON or VTT
209 whose principal neurons are glutamatergic, our histochemical analyses showed that the
210 majority of the neurons in this region were GABAergic, indicating that the
211 retrogradely-labelled GABAergic projection neurons are distinct from glutamatergic
212 projection neurons in the AON and VTT. We therefore temporarily named this region
213 with GABAergic projection neurons the ventral olfactory nucleus (VON) which was
214 located just beneath the AON. Then we examined neuroanatomical features of the VON.

215 It might be possible that the VON neurons are anteriorly displaced GABAergic
216 medium spiny neurons of the OT and NAc because the location of the VON is just
217 above the anterior tip of the OT and anterior to the NAc (Fig. 3). To examine this
218 possibility, we performed immunostaining for DARPP-32 and found that the strongly
219 immunoreactive OT and NAc neurons are clearly distinguishable from the less

220 immunoreactive VON neurons (Figs. 3 and 4).

221 Fluorescent labelling confirmed synaptic contacts between M/TCs in the OB
222 and VON neurons (Figs. 4 and 5). The dendrites of VON neurons projected in an
223 antero-ventral direction toward the cortical surface and extended through the layer Ia of
224 the olfactory cortex, where the dendrites were contacted by axons of M/TCs (Fig. 4).
225 Dendritic spines of VON neurons were apposed to immunoreactive VGlut1 elements in
226 the axons of M/TCs (Fig. 5). In addition to morphological analysis using retrograde
227 AAV encoding EGFP and tdTomato-expressing transgenic mice, we used a modified
228 rabies virus to demonstrate that M/TC axons form synaptic contacts with the VON
229 neurons (Fig. 6). Taking advantage of the neuronal pathway-specific infection of the
230 rabies virus combining retrograde Cre viral vectors and Cre-dependent expression of
231 viral receptors and glycoproteins²⁶, we successfully infected VON neurons with the
232 modified rabies virus. We observed that M/TCs in the OB were labelled by this
233 retrograde trans-synaptic method. These results confirmed that the VON is a part of the
234 olfactory cortex receiving axonal inputs from M/TCs.

235 The disynaptic pathway from the OB to the LH via the VON seems to be one
236 of shortcut pathways conveying odorant information to the LH. Unfortunately, the
237 efficacy of our rabies virus mediated-labelling of presynaptic M/TCs was insufficient to
238 address whether topographic axonal projections from the OB to the VON existed, as for
239 other subregions of the olfactory cortex²⁹. It remains to be addressed what odorant
240 information the VON conveys to the LH via GABAergic outputs. In addition to the OB,
241 the VON receives inputs from other regions of the olfactory cortex including the AON,
242 APC, OT, and PPC, as well as modulatory inputs from the horizontal limb of the
243 diagonal band, and top-down inputs from the prefrontal cortex (Fig. 6C). This

244 organization suggests that VON neurons integrate these inputs and send GABAergic
245 inhibitory output to the LH. Further studies should address the roles of each input to the
246 VON neurons and how the VON neurons integrates these inputs.

247 Rabies virus-mediated trans-synaptic labelling from the LH suggested that
248 VON neurons formed synaptic contacts in the LH (Fig. 7). The LH consists of a variety
249 of neuronal subtypes including orexin neurons, MCH neurons, and GABAergic neurons,
250 which have distinct roles in eating as well as sleep/wakefulness^{12,13,30}. It was recently
251 reported that medium spiny neurons in the NAc expressing dopamine receptor D1 have
252 synaptic inputs to GABAergic neurons in the LH³¹. This NAc to LH pathway is
253 involved in downregulation of feeding behaviour. Because our analysis did not identify
254 the neuronal subtypes in the LH that receive GABAergic inputs from the VON, further
255 neuroanatomical studies should address this point. In addition to anatomical analyses,
256 functional manipulation by optogenetics and/or pharmacogenetics will help to reveal the
257 roles of the VON. Our findings regarding the VON provide novel insight into the
258 circuitry that may underpin odour-induced LH-related behaviours.

259

260 **Materials and Methods**

261 **Animals**

262 All experiments were conducted in accordance with the Guidelines for Animal
263 Experimentation in Neuroscience of the Japan Neuroscience Society and were approved
264 by the Experimental Animal Research Committee of University of Fukui and Doshisha
265 University. C57BL/6J male mice were purchased from Japan SLC. Homozygote
266 Pcdh21-nCre mice (C57BL/6Cr-Tg(Pcdh21-cre)BYoko RBRC02189, RIKEN BRC)¹⁸
267 and homozygote Ai14 mice (B6;129S6-Gt(ROSA)26Sortm14(CAG-tdTomato)Hze/J
268 007908, The Jackson Laboratory)¹⁷ were crossed. Male heterozygote mice for both
269 genes were used for experiments in Figs. 4 and 5. All animals were individually housed
270 after surgery with a 12/12 hour light/dark cycle. Food and water were available *ad*
271 *libitum*.

272

273 **Virus preparation**

274 For AAV vectors, AAVrg-CAG-GFP was a gift from Edward Boyden (Addgene viral
275 prep #37825-AAVrg). AAV2-CMV-GFPCre, AAV2-CAG-Flex-TVA-mCherry, and
276 AAV2-CAG-Flex-rabies G were packaged and concentrated to titres of 5.0×10^{13} , $3.3 \times$
277 10^{12} , and 1.3×10^{12} viral genomes/mL as previously reported³² using Addgene plasmids
278 AAV-GFP/Cre (gift from Fred Gage, #49056³³), CAG-Flex-TCB (gift from Liqun Luo,
279 #48332²³), and pAAV-CAG-FLEX-oG-WPRE-SV40pA (gift from Edward Callaway,
280 #74292²²), respectively.

281 For the rabies virus, we obtained EnvA-pseudotyped glycoprotein-deleted
282 rabies virus encoding EGFP (SAD-dG-EGFP+EnvA) from Gene Transfer, Targeting and
283 Therapeutics Facility of Salk Institute for Biological Studies at a titre of 2.9×10^7

284 TU/mL.

285 For the lentivirus, NeuRet-Cre was packaged and concentrated to a titre of 1.1
286 x 10¹² copies/mL as previously reported³².

287

288 **Stereotaxic surgery**

289 The stereotaxic surgeries were performed on mice aged 10-16 weeks. Mice were
290 anesthetized with a mixture of three anaesthetics (medetomidine, midazolam, and
291 butorphanol)³⁴, and then placed in a stereotaxic apparatus (Narishige, SR-5M). The
292 skull above the targeted areas was thinned with a dental drill and removed carefully.
293 Injections were conducted with a syringe pump (WPI, UltraMicroPump III) connected
294 to a Hamilton syringe (Hamilton, RN-1701), mounted glass micropipette with a tip
295 diameter of 50 µm connected by an adaptor (Hamilton, 55750-01).

296 For Figs. 1-3, we unilaterally injected 150 nL of CTB conjugated with Alexa
297 555 into the left LH with the following coordinates: A/P, -1.2 mm and M/L, 1.2 mm
298 from bregma; D/V, 4.8 mm from the brain surface. One week later, the mice were
299 deeply anaesthetised and fixed as described below.

300 For Figs. 4 and 5, we unilaterally injected 300 nL of AAVrg-CAG-EGFP into
301 the left LH of the double transgenic mice with the following coordinates: A/P, -1.2 mm
302 and M/L, 1.2 mm from bregma; DV, 4.8 mm from the brain surface. Two weeks later,
303 the mice were deeply anesthetized and fixed as described below.

304 For Fig. 6, we unilaterally injected 300 nL of NeuRet-Cre into the left LH and
305 300 nL of 1:1 mixture of two AAVs (AAV2-CAG-Flex-TVA-mCherry and
306 AAV2-CAG-Flex-rabies G) into the left VON. For the LH, we used the following
307 coordinates: A/P, -1.2 mm and M/L, 1.2 mm from bregma; DV, 4.8 mm from the brain

308 surface. For the VON, we used the following coordinates: A/P, +2.0 mm and M/L, 0.8
309 mm from bregma; DV, 4.2 mm from the brain surface. Two weeks later, we unilaterally
310 injected 300 nL of SAD-dG-EGFP+EnvA using the same VON coordinates. One week
311 later, the mice were deeply anaesthetised and fixed as described below.

312 For Fig. 7, we unilaterally injected 300 nL of 1:1:1 mixture of three AAVs
313 (AAV2-CMV-GFPCre, AAV2-CAG-Flex-TVA-mCherry, and AAV2-CAG-Flex-rabies
314 G) for rabies G(+) mice or 300 nL of 1:1 mixture of two AAVs (AAV2-CMV-GFPCre
315 and AAV2-CAG-Flex-TVA-mCherry) for rabies G(-) mice into the left LH with the
316 following coordinates: A/P, -1.2 mm and M/L, 1.2 mm from bregma; D/V, 4.8 mm from
317 the brain surface. Two weeks later, we unilaterally injected 300 nL of
318 SAD-dG-EGFP+EnvA using the same LH coordinates. One week later, the mice were
319 deeply anaesthetised and fixed as described below.

320

321 **Sample preparation for histochemistry**

322 Mice were deeply anaesthetised by intraperitoneal injection of sodium pentobarbital.
323 They were transcardially perfused with phosphate-buffered saline (PBS) followed by
324 4% paraformaldehyde (PFA). The brains were removed from the skull, immersed in 4%
325 PFA in 0.1 M phosphate buffer (PB) overnight, and then transferred to 30% sucrose in
326 0.1 M PB. The brains were then embedded in O.C.T. compound (Sakura Finetechical),
327 frozen at -80°C, and sliced into coronal sections with a thickness of 20 µm with a
328 cryotome. Sections were rinsed in PBS and 0.1 M PB, mounted on glass slides
329 (Matsunami, CREST) using a paint brush, dried overnight in a vacuum desiccator, and
330 then stored at 4°C until histochemistry.

331

332 **Histochemistry**

333 We performed immunostaining for orexin (Fig. 1A, middle), MCH (Fig. 1A, right),
334 DARPP-32 (Figs. 3, 4, and 7), EGFP (Figs. 4 and 5), and VGlut1 (Fig. 5) as follows.
335 The dried sections were rehydrated in PBS, permeabilised in TNT (0.1 M Tris-HCl; pH,
336 7.5; 0.15 M NaCl; 0.1% Tween 20), and blocked with 10% normal donkey serum
337 diluted in TNT. Then, the sections were incubated with the following primary antibodies
338 overnight at 4°C: goat anti-orexin polyclonal antibody (1:400; Santa Cruz sc-8070);
339 rabbit anti-MCH polyclonal antibody (1:400, Sigma M8440); rabbit anti-DARPP-32
340 monoclonal antibody (1:400; Abcam ab40801); rat anti-EGFP monoclonal antibody
341 (1:1000, Nacalai Tesque 04404-84); guinea pig anti-VGlut1 polyclonal antibody (1:500,
342 Merck AB5905). After three washes in TNT, appropriate fluorescent dye-conjugated
343 secondary antibodies (1:400; Jackson ImmunoResearch) were incubated for 2 hours at
344 room temperature. After three washes in TNT, the sections were then counterstained
345 with DAPI diluted in PBS (2 µg/mL) for 5 min. After washing in PBS, the sections were
346 mounted in PermaFluor (Thermo Fisher Scientific).

347 For Fig. 2A, we performed *in situ* hybridization for VGlut1, VGlut2, VGlut3,
348 and GAD65/67 mRNA as follows. Digoxigenin (DIG)-labelled RNA probes were made
349 using an *in vitro* transcription kit (Roche) according to the manufacturer's protocol with
350 plasmids kindly provided by Drs. Katsuhiko Ono and Yuchio Yanagawa³⁵⁻³⁷. The dried
351 sections were fixed in 4% PFA, digested with Proteinase K (10 µg/mL) for 30 min, and
352 post-fixed in 4% PFA. After prehybridization, the sections were incubated overnight at
353 65°C with DIG-labelled RNA probes. After stringent washing, the sections were
354 blocked with 10% normal sheep serum, 1% bovine serum albumin (BSA), and 0.1%
355 Triton X-100 in PBS. Subsequently, the sections were incubated overnight at 4°C with

356 alkaline phosphatase-conjugated anti-DIG antibody (1:1000; Roche). The sections were
357 washed in TNT, followed by alkaline phosphatase buffer (100 mM NaCl; 100 mM
358 Tris-HCl; pH, 9.5; 50 mM MgCl₂; 0.1% Tween 20; 5 mM levamisole). The sections
359 were treated overnight with NBT/BCIP (Roche) mixture at room temperature in a dark
360 room for colour development. Then, they were rinsed in PBS and mounted in
361 PermaFluor (Thermo Fisher Scientific).

362 For Fig. 2B, we performed double fluorescent labelling of immunoreactivity
363 for CTB and mRNA for VGluT1 or GAD65/67 as follows. Fluorescein-labelled RNA
364 probes were prepared as described above. Hybridization and washing were performed as
365 described above, except that fluorescein-labelled probes were used for hybridization.
366 After blocking in 1% blocking buffer (11096176001, Roche) for 1 h, the
367 fluorescent-labelled probes were detected. The sections were incubated with an
368 anti-fluorescein antibody conjugated with horseradish peroxidase (1:500; Perkin-Elmer)
369 for 1 h at room temperature. After three 10-min washes in TNT, the sections were
370 treated with diluted (1:100) TSA-Plus dinitrophenol (DNP) reagents for 5 min
371 according to the manufacturer's instructions (Perkin-Elmer), and the FLU signals were
372 converted to DNP signals. To amplify the DNP signals, the sections were washed in
373 TNT three times for 10 min each, incubated with an anti-DNP antibody conjugated with
374 horseradish peroxidase (1:500; Perkin-Elmer) for 1 h at room temperature, and treated
375 again with diluted TSA-Plus DNP reagents (1:100) for 5 min. Subsequently, the sections
376 were incubated overnight with an anti-DNP antibody conjugated with Alexa 488 (1:500;
377 Molecular Probes) in 1% blocking buffer at 4°C for fluorescence detection of DNP
378 signals. At this point, a goat anti-CTB antibody (1:500; List Biological Laboratories
379 #703) was added to the incubation mixture for detection of CTB. The sections were

380 washed three times in TNT and incubated with a Cy3-conjugated secondary antibody
381 (1:400; Jackson ImmunoResearch Labs) for 2 h. After three washes in TNT, the sections
382 were then counterstained with DAPI diluted in PBS (2 μ g/mL) for 5 min. After washing
383 in PBS, the sections were mounted in PermaFluor (Thermo Fisher Scientific).

384 For Figs. 1A (left panel), 1B, 2A (two left panels), and 6, the dried sections
385 were rehydrated in PBS and counterstained with DAPI diluted in PBS (2 μ g/mL) for 5
386 min. After washing in PBS, the sections were mounted in PermaFluor (Thermo Fisher
387 Scientific).

388

389 **Microscopy**

390 Sections were examined with a bright field virtual slide system (Hamamatsu Photonics,
391 NanoZoomer), a fluorescent microscope (Olympus, BX51WI), and a confocal laser
392 microscope (Olympus, FV1200).

393

394 **Availability of Materials and Data**

395 In publication we make materials, data and associated protocols promptly available to
396 readers without undue qualifications in material transfer agreements.

397

398 **References**

399 1 Doty, R. L. Odor-guided behavior in mammals. *Experientia* 42, 257-271
400 (1986).

401 2 Kobayakawa, K. et al. Innate versus learned odour processing in the mouse
402 olfactory bulb. *Nature* 450, 503-508, doi:10.1038/nature06281 (2007).

403 3 Saito, H. et al. Immobility responses are induced by photoactivation of single
404 glomerular species responsive to fox odour TMT. *Nat Commun* 8, 16011,
405 doi:10.1038/ncomms16011 (2017).

406 4 Inokuchi, K. et al. Nrp2 is sufficient to instruct circuit formation of mitral-cells
407 to mediate odour-induced attractive social responses. *Nat Commun* 8, 15977,
408 doi:10.1038/ncomms15977 (2017).

409 5 Mori, K. & Sakano, H. How Is the Olfactory Map Formed and Interpreted in
410 the Mammalian Brain? *Annu Rev Neurosci* 34, 467-499,
411 doi:10.1146/annurev-neuro-112210-112917 (2011).

412 6 Shepherd, G. M. *The Synaptic Organization of the Brain.* (Oxford University
413 Press, 2004).

414 7 Murata, K., Kanno, M., Ieki, N., Mori, K. & Yamaguchi, M. Mapping of
415 Learned Odor-Induced Motivated Behaviors in the Mouse Olfactory Tubercl. *J
416 Neurosci* 35, 10581-10599, doi:10.1523/JNEUROSCI.0073-15.2015 (2015).

417 8 Anand, B. K. & Brobeck, J. R. Hypothalamic control of food intake in rats and
418 cats. *Yale J Biol Med* 24, 123-140 (1951).

419 9 Petrovich, G. D. Lateral Hypothalamus as a Motivation-Cognition Interface in
420 the Control of Feeding Behavior. *Front Syst Neurosci* 12, doi:ARTN 14
421 10.3389/fnsys.2018.00014 (2018).

422 10 Groenewegen, H. J., Berendse, H. W. & Haber, S. N. Organization of the
423 output of the ventral striatopallidal system in the rat: ventral pallidal efferents.
424 Neuroscience 57, 113-142 (1993).

425 11 Price, J. L., Slotnick, B. M. & Revial, M. F. Olfactory projections to the
426 hypothalamus. J Comp Neurol 306, 447-461, doi:10.1002/cne.903060309 (1991).

427 12 Barson, J. R., Morganstern, I. & Leibowitz, S. F. Complementary roles of
428 orexin and melanin-concentrating hormone in feeding behavior. Int J Endocrinol 2013,
429 983964, doi:10.1155/2013/983964 (2013).

430 13 Sakurai, T. Roles of orexins in the regulation of body weight homeostasis.
431 Obes Res Clin Pract 8, e414-420, doi:10.1016/j.orcp.2013.12.001 (2014).

432 14 Chang, H. T. & Kitai, S. T. Projection neurons of the nucleus accumbens: an
433 intracellular labeling study. Brain Res 347, 112-116 (1985).

434 15 Millhouse, O. E. & Heimer, L. Cell configurations in the olfactory tubercle of
435 the rat. J Comp Neurol 228, 571-597, doi:10.1002/cne.902280409 (1984).

436 16 Ouimet, C. C., Miller, P. E., Hemmings, H. C., Jr., Walaas, S. I. & Greengard,
437 P. DARPP-32, a dopamine- and adenosine 3':5'-monophosphate-regulated
438 phosphoprotein enriched in dopamine-innervated brain regions. III.
439 Immunocytochemical localization. J Neurosci 4, 111-124 (1984).

440 17 Madisen, L. et al. A robust and high-throughput Cre reporting and
441 characterization system for the whole mouse brain. Nat Neurosci 13, 133-140,
442 doi:10.1038/nn.2467 (2010).

443 18 Nagai, Y., Sano, H. & Yokoi, M. Transgenic expression of Cre recombinase in
444 mitral/tufted cells of the olfactory bulb. Genesis 43, 12-16, doi:10.1002/gene.20146
445 (2005).

446 19 Tervo, D. G. et al. A Designer AAV Variant Permits Efficient Retrograde
447 Access to Projection Neurons. *Neuron* 92, 372-382, doi:10.1016/j.neuron.2016.09.021
448 (2016).

449 20 Kaneko, T., Fujiyama, F. & Hioki, H. Immunohistochemical localization of
450 candidates for vesicular glutamate transporters in the rat brain. *J Comp Neurol* 444,
451 39-62 (2002).

452 21 Ohmomo, H. et al. Temporally distinct expression of vesicular glutamate
453 transporters 1 and 2 during embryonic development of the rat olfactory system.
454 *Neurosci Res* 70, 376-382, doi:10.1016/j.neures.2011.05.005 (2011).

455 22 Kim, E. J., Jacobs, M. W., Ito-Cole, T. & Callaway, E. M. Improved
456 Monosynaptic Neural Circuit Tracing Using Engineered Rabies Virus Glycoproteins.
457 *Cell Rep* 15, 692-699, doi:10.1016/j.celrep.2016.03.067 (2016).

458 23 Miyamichi, K. et al. Dissecting local circuits: parvalbumin interneurons
459 underlie broad feedback control of olfactory bulb output. *Neuron* 80, 1232-1245,
460 doi:10.1016/j.neuron.2013.08.027 (2013).

461 24 Watabe-Uchida, M., Zhu, L., Ogawa, S. K., Vamanrao, A. & Uchida, N.
462 Whole-brain mapping of direct inputs to midbrain dopamine neurons. *Neuron* 74,
463 858-873, doi:10.1016/j.neuron.2012.03.017 (2012).

464 25 Wickersham, I. R. et al. Monosynaptic restriction of transsynaptic tracing from
465 single, genetically targeted neurons. *Neuron* 53, 639-647,
466 doi:10.1016/j.neuron.2007.01.033 (2007).

467 26 Schwarz, L. A. et al. Viral-genetic tracing of the input-output organization of a
468 central noradrenaline circuit. *Nature* 524, 88-92, doi:10.1038/nature14600 (2015).

469 27 Kobayashi, K. et al. Pseudotyped Lentiviral Vectors for Retrograde Gene

470 1 Delivery into Target Brain Regions. *Frontiers in Neuroanatomy* 11, doi:ARTN 65
471 10.3389/fnana.2017.00065 (2017).

472 28 Chen, S. & Astonjones, G. Evidence That Cholera-Toxin-B Subunit (Ctb) Can
473 Be Avidly Taken up and Transported by Fibers of Passage. *Brain Research* 674,
474 107-111, doi:Doi 10.1016/0006-8993(95)00020-Q (1995).

475 29 Miyamichi, K. et al. Cortical representations of olfactory input by
476 trans-synaptic tracing. *Nature* 472, 191-196, doi:10.1038/nature09714 (2011).

477 30 Wu, Z. et al. GABAergic projections from lateral hypothalamus to
478 paraventricular hypothalamic nucleus promote feeding. *J Neurosci* 35, 3312-3318,
479 doi:10.1523/JNEUROSCI.3720-14.2015 (2015).

480 31 O'Connor, E. C. et al. Accumbal D1R Neurons Projecting to Lateral
481 Hypothalamus Authorize Feeding. *Neuron* 88, 553-564,
482 doi:10.1016/j.neuron.2015.09.038 (2015).

483 32 Kobayashi, K. et al. Survival of corticostriatal neurons by Rho/Rho-kinase
484 signaling pathway. *Neurosci Lett* 630, 45-52, doi:10.1016/j.neulet.2016.07.020 (2016).

485 33 Kaspar, B. K. et al. Adeno-associated virus effectively mediates conditional
486 gene modification in the brain. *Proc Natl Acad Sci U S A* 99, 2320-2325,
487 doi:10.1073/pnas.042678699 (2002).

488 34 Nakamura, T. et al. Effects of a mixture of medetomidine, midazolam and
489 butorphanol on anesthesia and blood biochemistry and the antagonizing action of
490 atipamezole in hamsters. *J Vet Med Sci* 79, 1230-1235, doi:10.1292/jvms.17-0210
491 (2017).

492 35 Asada, H. et al. Cleft palate and decreased brain gamma-aminobutyric acid in
493 mice lacking the 67-kDa isoform of glutamic acid decarboxylase. *Proc Natl Acad Sci U*

494 36 S A 94, 6496-6499 (1997).

495 36 Makinae, K. et al. Structure of the mouse glutamate decarboxylase 65 gene and
496 its promoter: preferential expression of its promoter in the GABAergic neurons of
497 transgenic mice. J Neurochem 75, 1429-1437 (2000).

498 37 Ono, K. et al. Regional- and temporal-dependent changes in the differentiation
499 of Olig2 progenitors in the forebrain, and the impact on astrocyte development in the
500 dorsal pallium. Dev Biol 320, 456-468, doi:10.1016/j.ydbio.2008.06.001 (2008).

501

502 **Acknowledgements**

503 We thank Drs. Edward Callaway, Fumitaka Osakada, and Akihiro Yamanaka for
504 providing viral vectors and valuable discussion, Drs. Katsuhiko Ono and Yuchio
505 Yanagawa for plasmids for RNA probes, Eri Murai, Noriko Funabashi, and members of
506 the Fukazawa laboratory and Life Science Research Laboratory at University of Fukui
507 for technical assistance. K.Murata was supported by the Takeda Science Foundation,
508 Cosmetology Research Foundation, and JSPS KAKENHI Grant Numbers 16K18377,
509 16H01671, 17KK0190, 18H05005. Y.F. was supported by JSPS KAKENHI Grant
510 Numbers 15H01282, 16H04662. H.M. was supported by the Takeda Science
511 Foundation, Urakami Foundation for Food and Food Culture Promotion and JSPS
512 KAKENHI Grant Numbers 16K14557, 16H02061.

513

514 **Author Contributions**

515 K.Murata and H.M. designed research, performed experiments, analysed data, and
516 wrote the paper. T.K. performed experiments. Y.F., Kenta.K., Kazuto K., K.Miyamichi,
517 H.O., H.B., Y.S., M.Y., and K. Mori contributed to reagents and commented on the
518 manuscript.

519

520 **Competing interests**

521 The authors declare no competing interests.

522

523 **Figure Legends**

524 **Figure 1 Retrograde tracer revealed a cluster of neurons projecting to the lateral
525 hypothalamus (LH) surrounded by the olfactory cortex.**

526 (A) Coronal sections of the LH after injection of Alexa 555-conjugated cholera toxin B
527 subunit (CTB, red) with DAPI staining (blue). Immunostaining for orexin (middle,
528 green) or melanin-concentrating hormone (MCH) (right, green) was performed. Scale
529 bars: 200 μ m in left panel, 100 μ m in middle and right panels. 3V, third ventricle. (B)
530 CTB-labelled cells in the frontal cortex and olfactory cortex. The inset in the left panel
531 is magnified in the right panel. APC, anterior piriform cortex; AON, anterior olfactory
532 nucleus; VTT, ventral tenia tecta; OT, olfactory tubercle. Scale bars: 500 μ m in left
533 panel, 100 μ m in right panel.

534

535 **Figure 2 Majority of CTB-labelled neurons in the ventral olfactory nucleus (VON)
536 were GABAergic.**

537 (A) *In situ* hybridization for VGlUTs and GAD65/67 mRNAs, and adjacent slice images
538 of cholera toxin B subunit (CTB)-labelled ventral olfactory nucleus (VON) neurons.
539 Scale bars: 100 μ m. (B) Double fluorescent labelling of CTB and VGlUT1 (upper
540 panels) or GAD65/67 (lower panels) mRNAs with DAPI staining. Scale bar: 100 μ m.

541

542 **Figure 3 The VON was distinguishable from the ventral striatum by DARPP-32
543 immunoreactivity.**

544 (A and B) Coronal sections (A) and sagittal sections (B) of the VON after injection of
545 Alexa 555-conjugated cholera toxin B subunit (CTB) (red) into the lateral hypothalamus
546 (LH) with immunostaining for DARPP-32 (green) and DAPI staining (blue). AON,

547 anterior olfactory nucleus; VON, ventral olfactory nucleus; OT, olfactory tubercle; NAc,
548 nucleus accumbens. Scale bars: 100 μ m.

549

550 **Figure 4 Mitral and tufted cells in the olfactory bulb send axons to the VON**

551 (A) Sagittal sections of the whole brain of the mitral and tufted cells (M/TCs) in a
552 tdTomato-labelled transgenic mouse after injection of retrograde adeno-associated virus
553 (AAV) vector encoding EGFP into the lateral hypothalamus (LH). The inset of the left
554 panel is magnified in the right panel. We note that vascular endothelial cells and some
555 neurons in the olfactory cortex were labelled by tdTomato as well as M/TCs. Scale bars:
556 1 mm in left panel, 100 μ m in right panel. (B) Sagittal sections of the ventral olfactory
557 nucleus (VON) with immunostaining for DARPP-32 (blue). Dendrites of
558 EGFP-labelled VON neurons (green) innervated layer Ia of the olfactory cortex which
559 was innervated by axons of tdTomato-labelled M/TCs (red). Scale bar: 100 μ m.

560

561 **Figure 5 Synaptic contacts between mitral and tufted cells and spines of neurons in**
562 **the VON**

563 Single place confocal images of dendrites of EGFP-labelled ventral olfactory nucleus
564 (VON) neurons (green), axons of tdTomato-labelled mitral and tufted cells (M/TCs)
565 (red) and immunoreactivity for vesicular glutamate transporter 1 (VGluT1) (blue) in
566 layer Ia of the VON. Lower four panels are magnified views of the inset. Scale bars: 20
567 μ m for upper four panels, 5 μ m for lower four panels.

568

569 **Figure 6 Rabies virus-mediated trans-synaptic retrograde tracing from the VON**

570 (A) Schema of virus-mediated neuronal pathway-specific retrograde tracing. We first
571 injected a retrograde lentiviral vector coding Cre (NeuRet-Cre) into the lateral
572 hypothalamus (LH), and Cre-dependent adeno-associated virus (AAV) vector
573 TVA-mCherry and rabies G into the VON. Two weeks after the first injection,
574 EnvA-pseudotyped glycoprotein-deleted rabies virus encoding EGFP was injected into
575 the VON. We then observed distribution of EGFP-labelled presynaptic cells throughout
576 the whole brain. (B) Coronal sections of the VON. Left, TVA-mCherry expressing
577 neurons; middle, rabies-derived EGFP expressing neurons; right, colour merged with
578 DAPI staining. Yellow cells are TVA-mCherry(+) EGFP(+) starter cells. AON, anterior
579 olfactory nucleus; VON, ventral olfactory nucleus; OT, olfactory tubercle. Scale bar:
580 100 μ m. (C) Distribution of EGFP-labelled presynaptic cells to the VON. GCL, granule
581 cell layer; MCL, mitral cell layer; EPL, external plexiform layer; GL, glomerular layer;
582 AON, anterior olfactory nucleus; APC, anterior piriform cortex; OFC, orbitofrontal
583 cortex; mPFC, medial prefrontal cortex; HDB, horizontal limb of the diagonal band; OT,
584 olfactory tubercle; PPC, posterior piriform cortex. Scale bar: 100 μ m.

585

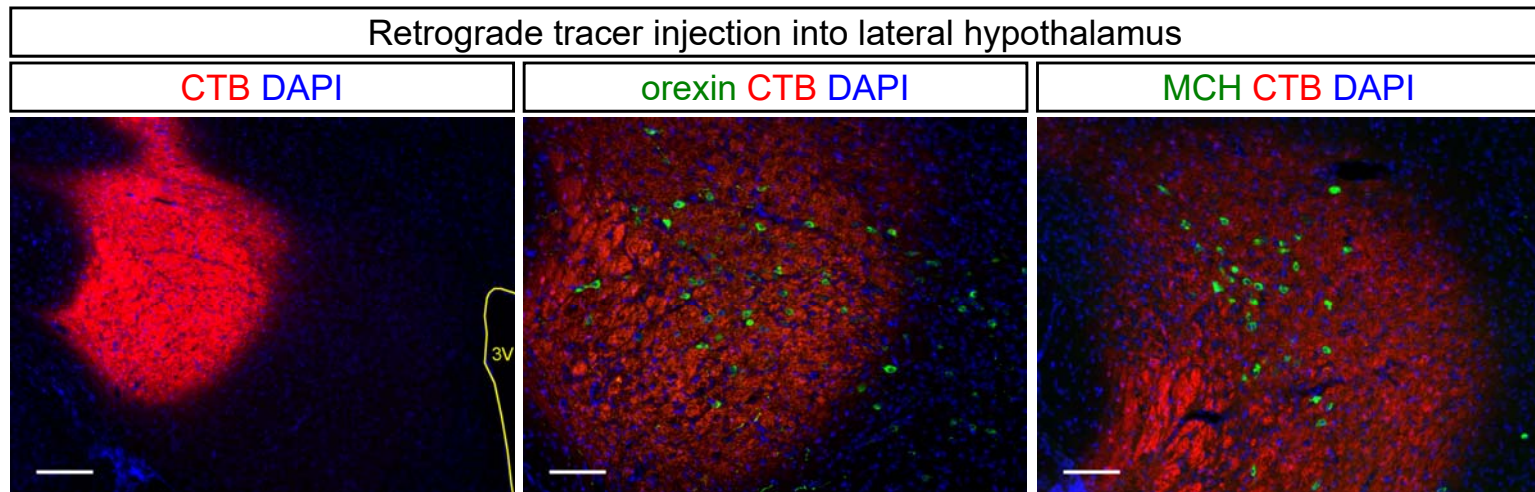
586 **Figure 7 Trans-synaptic retrograde spread of rabies virus from the LH to the VON**

587 (A) Schema of virus-mediated retrograde tracing. We first injected a mixture of
588 adeno-associated viruses (AAVs) encoding CMV-GFPCre and
589 CAG-Flex-TVA-mCherry either with or without CAG-Flex-rabies G into the lateral
590 hypothalamus (LH). Two weeks later, SAD-dG-EGFP-EnvA was injected into the LH
591 and we observed the distribution of EGFP-labelled presynaptic cells in the ventral
592 olfactory nucleus (VON). (B) EGFP-labelled presynaptic neurons (left, green) were
593 observed in the VON when rabies G-encoding AAV was concomitantly injected (upper

594 panels). Immunostaining for DARPP-32 (middle, red) was used to discriminate the
595 VON from the olfactory tubercle (OT) and nucleus accumbens (NAc). Scale bar: 100
596 μ m.

Figure 1

A



B

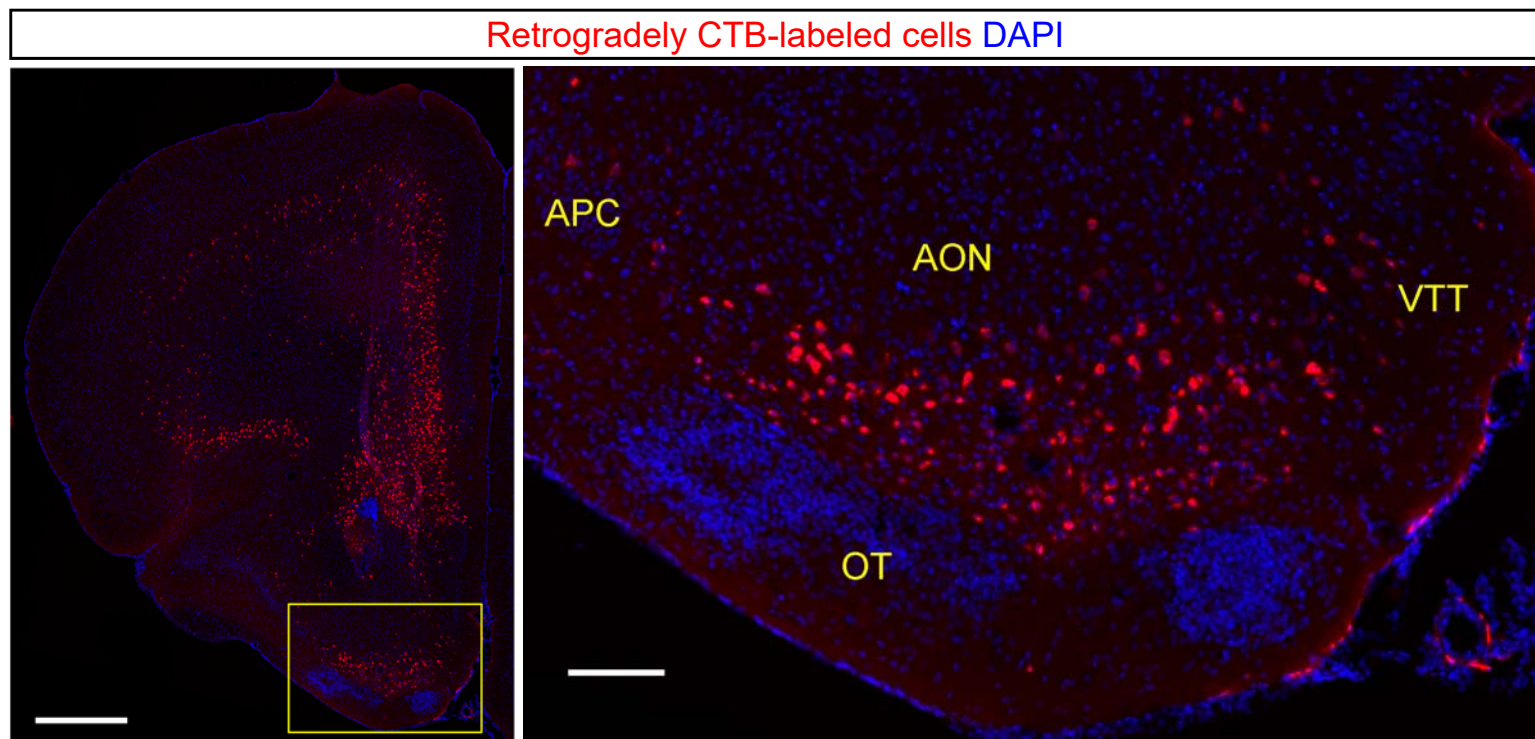
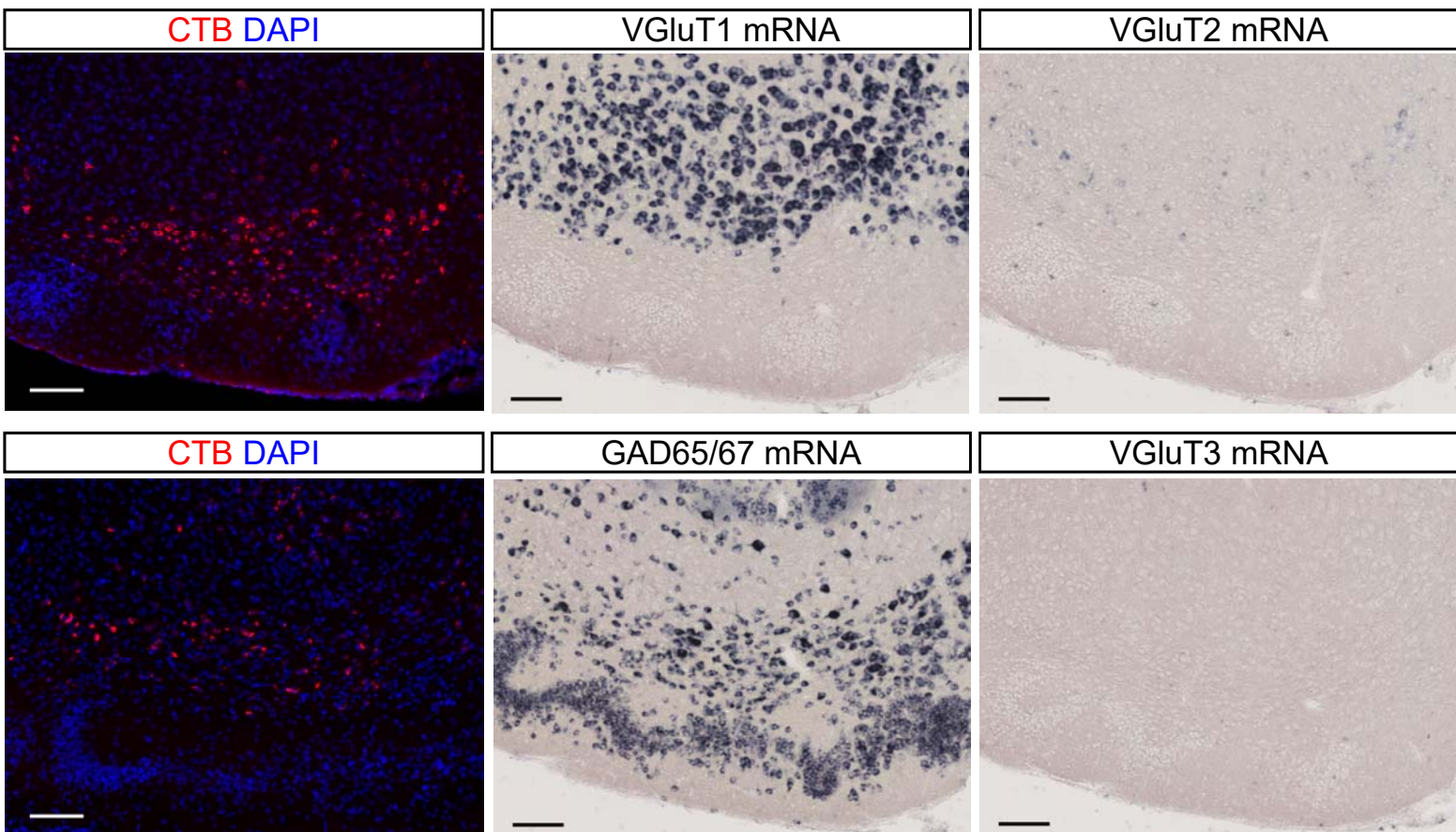


Figure 2

A



B

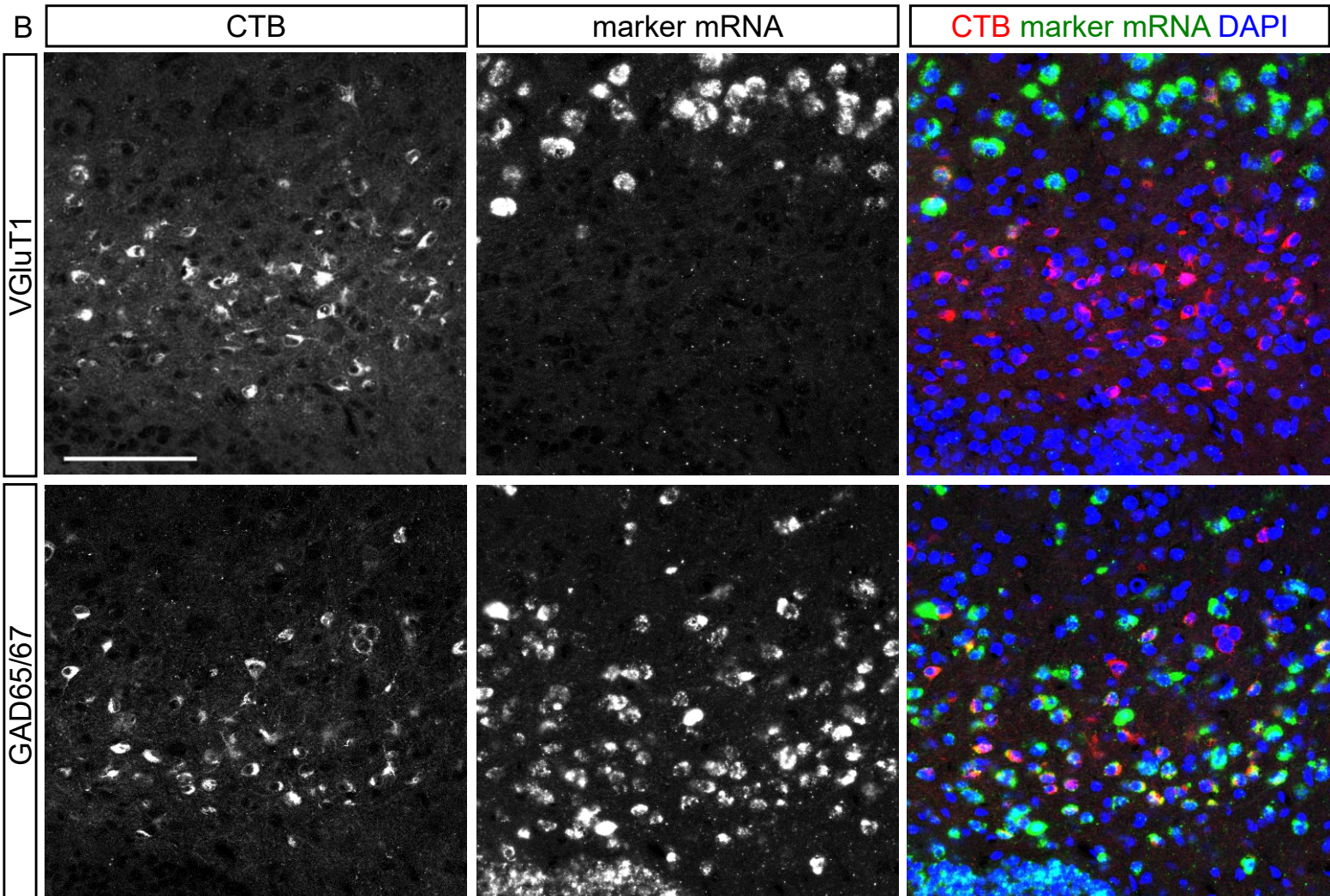


Figure 3

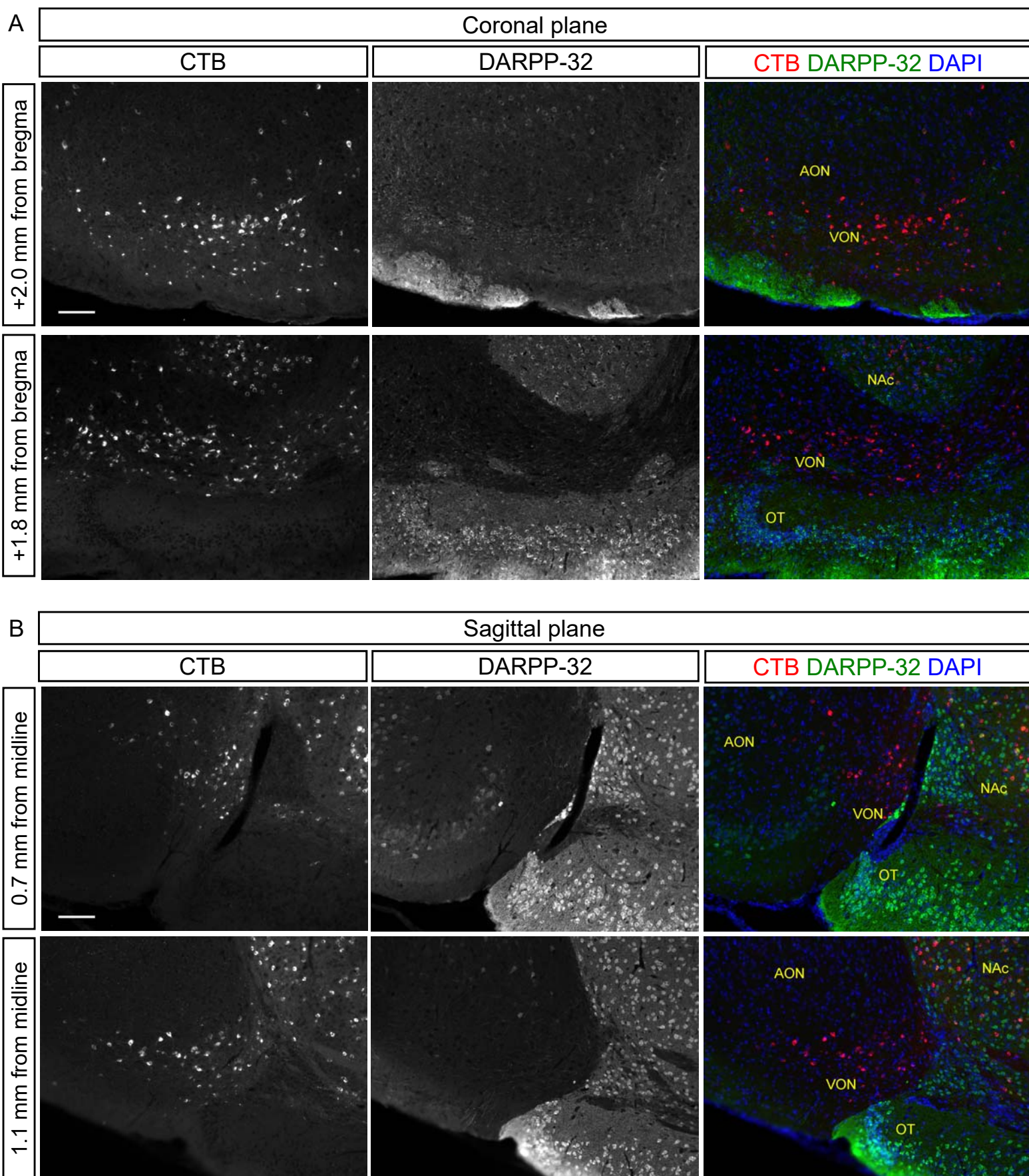
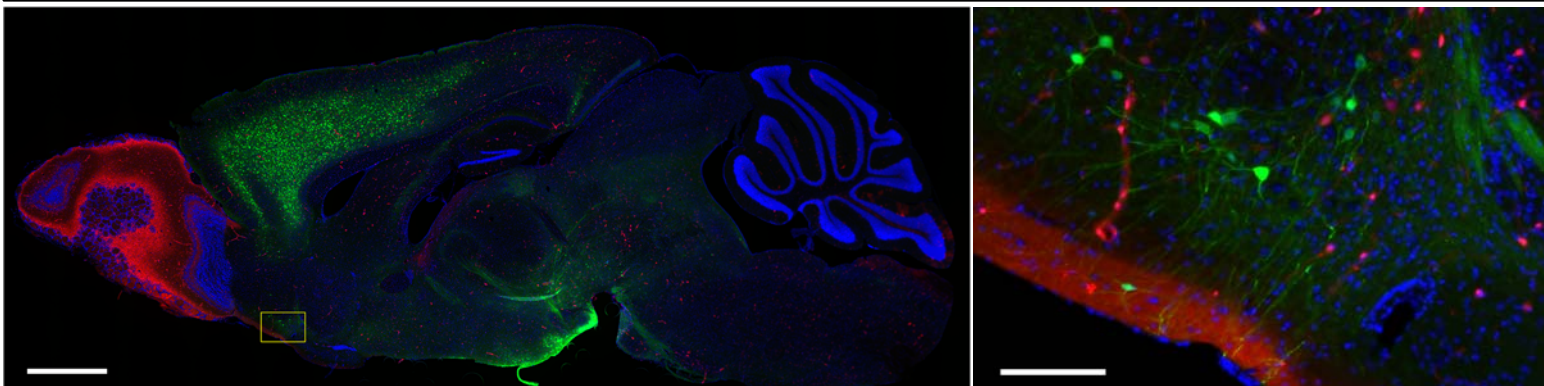


Figure 4

A

Pcdh21-nCre;Ai14 (tdTomato Cre reporter) mouse AAVrg-CAG-EGFP into LH DAPI



B

Sagittal plane

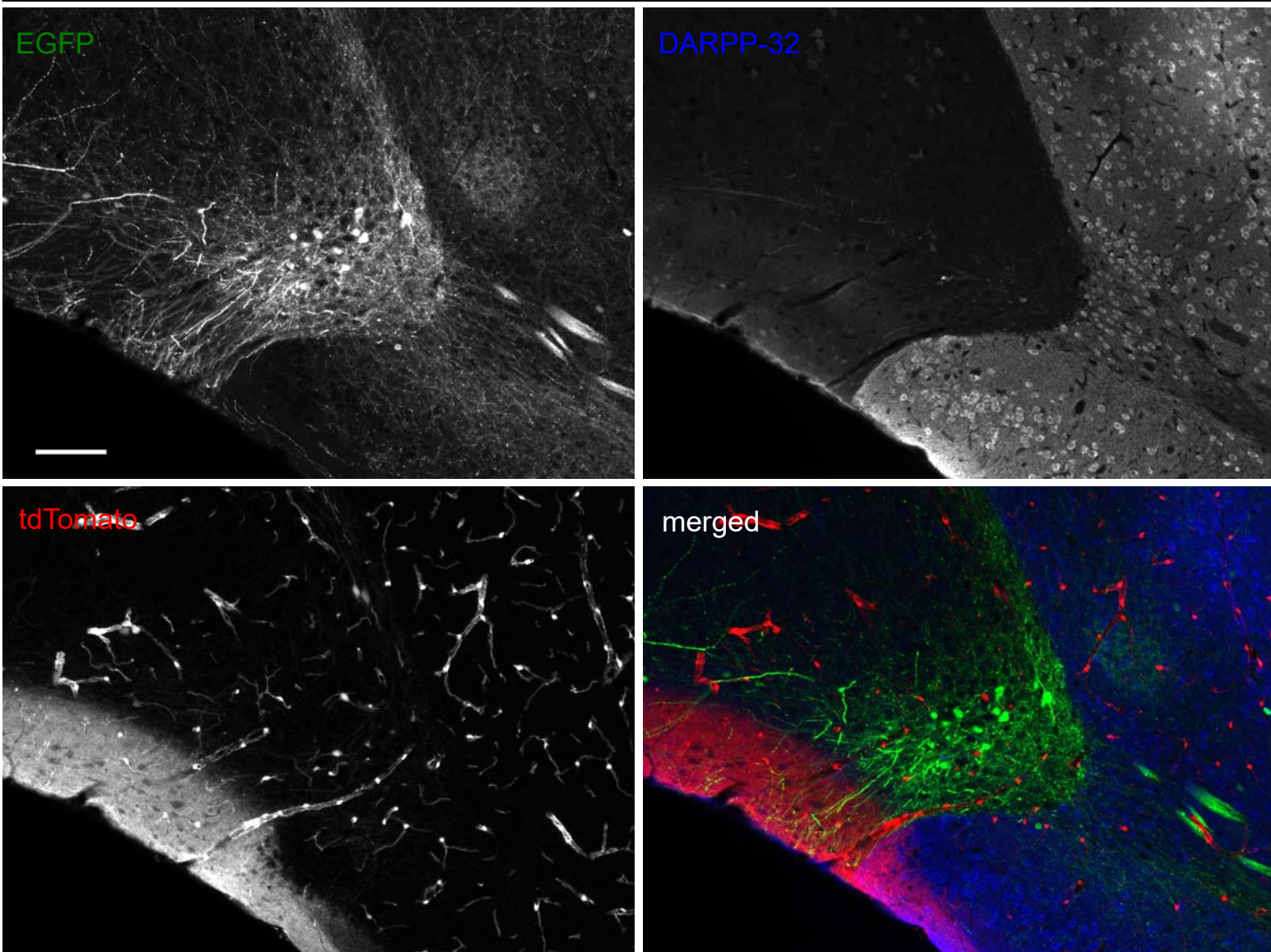


Figure 5

Synapses between M/TC axons and dendrites of VON neurons (coronal, single Z plane)

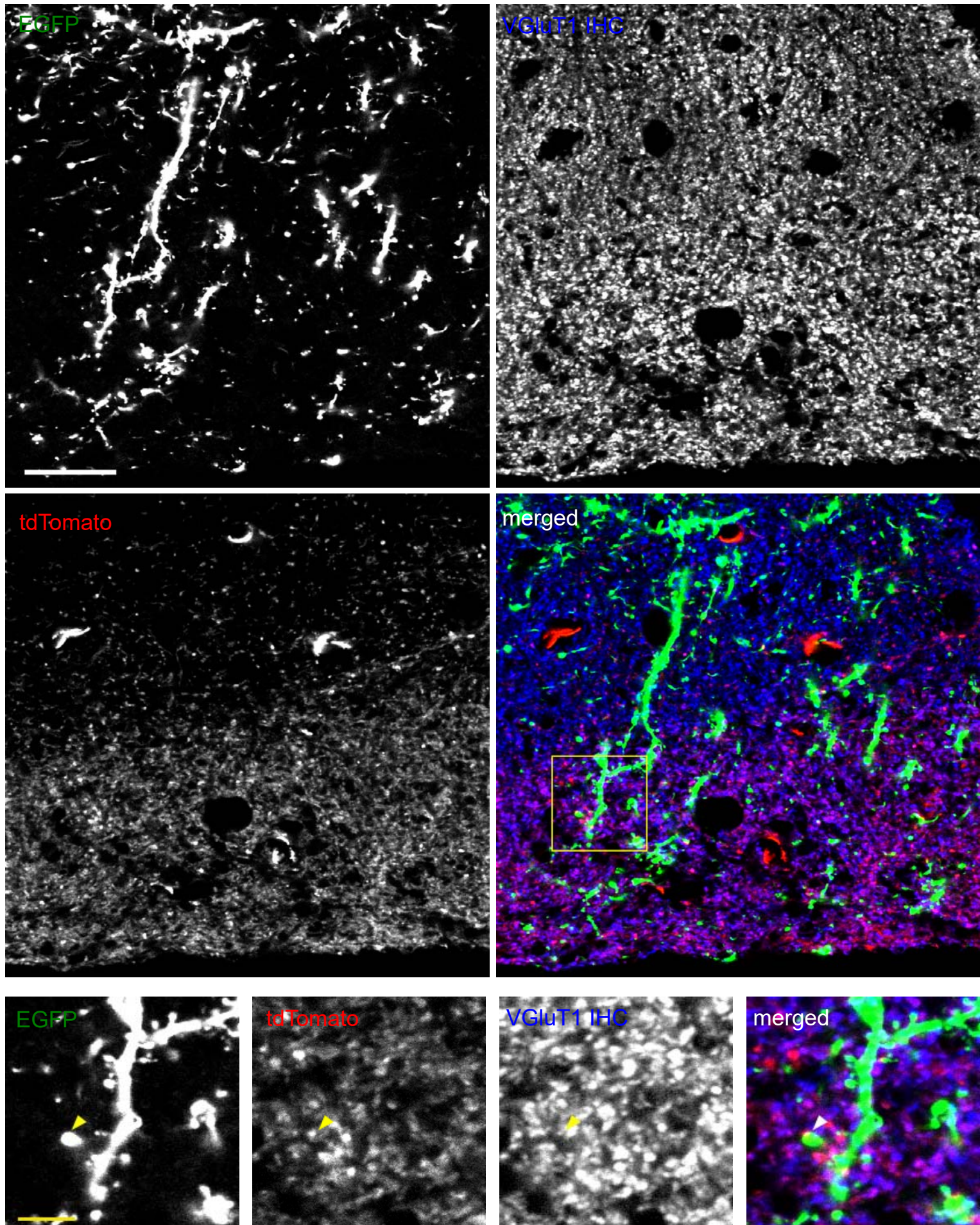


Figure 6

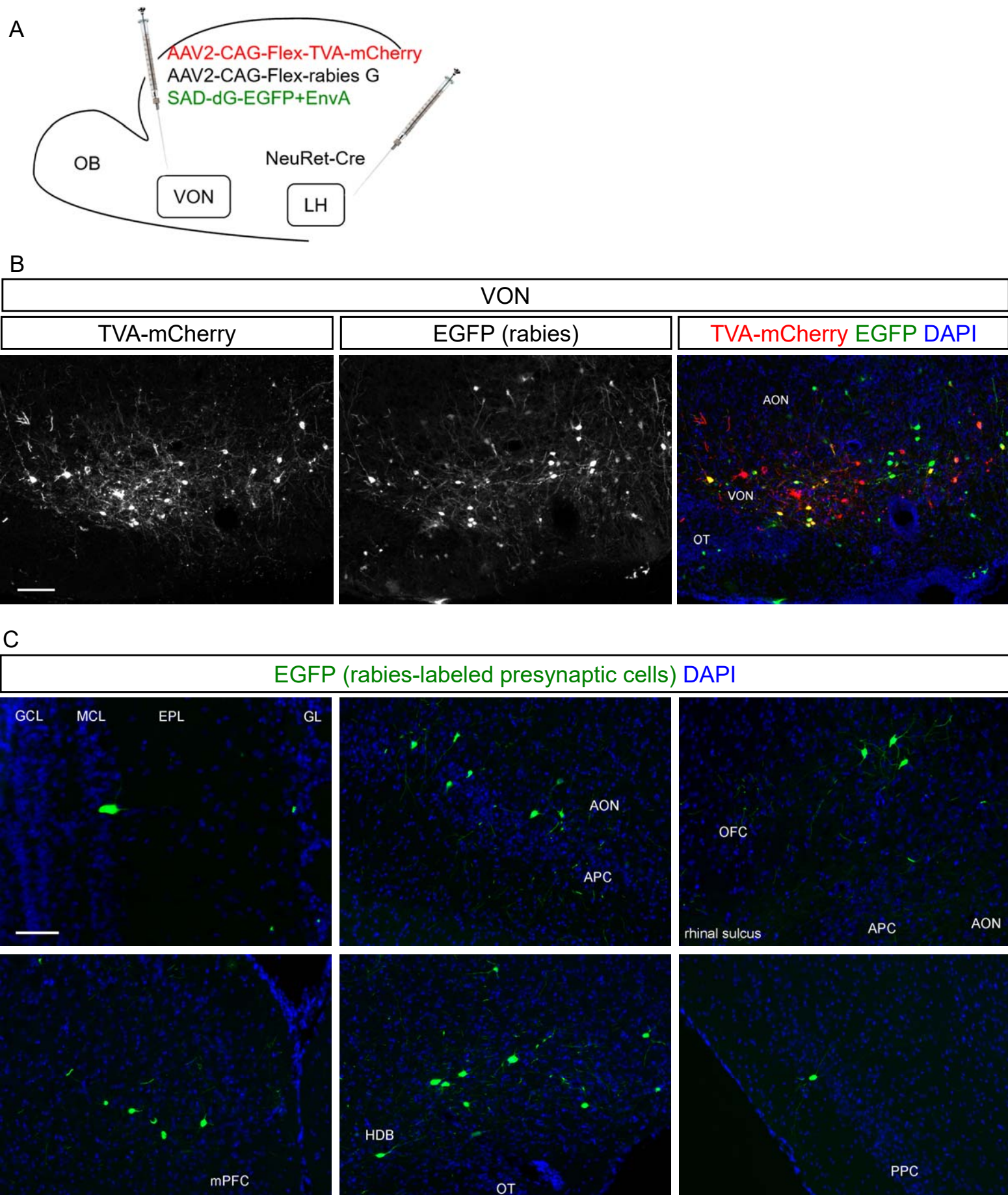
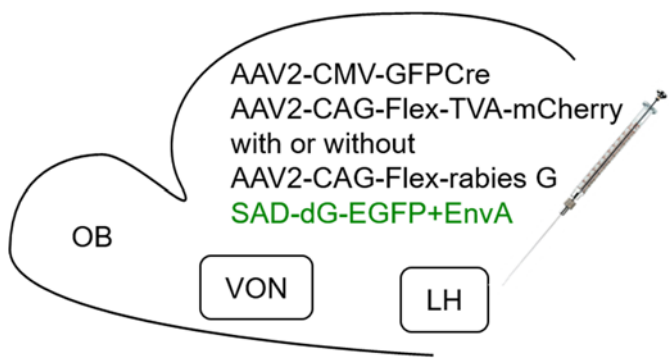


Figure 7

A



B

